

1 **Deceiving The Big Eaters: *Salmonella* Typhimurium**
2 **SopB subverts host cell Xenophagy through Akt-**
3 **TFEB axis in macrophages**

4 Ritika Chatterjee ¹, Debalina Chaudhuri ¹, Subba Rao Gangi
5 Setty ¹ and Dipshikha Chakravortty ^{1,2*}

6 1 Department of Microbiology and Cell Biology, Division of Biological Sciences,
7 Indian Institute of Science, Bengaluru, India

8 2 Centre for Biosystems Science and Engineering, Indian Institute of Science,
9 Bengaluru, India

10

11 Current address: Department of Microbiology and Cell Biology, Indian Institute of Science,
12 Bangalore, Karnataka, India-560012

13 * Corresponding author

14 Dipshikha Chakravortty

15 Email: dipa@ iisc.ac.in

16 Tel: 0091 80 2293 2842

17 Fax: 0091 80 2360 269

18

19 **ABSTRACT:**

20 *Salmonella*, a stealthy facultative intracellular pathogen, harbors an array of host immune
21 evasion strategies. This facilitates successful survival and replicative niches establishment in
22 otherwise hostile host innate immune cells such as macrophages. *Salmonella* survives and
23 utilizes macrophages for effective dissemination throughout the host causing systemic
24 infection. One of the central host defense mechanisms in macrophages is bacterial xenophagy
25 or macro-autophagy. Here we report for the first time that *Salmonella* pathogenicity island-1
26 (SPI-1) effector SopB is involved in subverting host autophagy through dual mechanisms.
27 SopB is known to act as a phosphoinositide phosphatase and thereby can alter the
28 phosphoinositide dynamics of the host cell. Here we demonstrate that this activity helps the
29 bacterium escape autophagy by inhibiting terminal fusion of *Salmonella* containing vacuole
30 (SCV) with both lysosomes and autophagosomes. We also report the second mechanism,
31 wherein SopB downregulates overall lysosomal biogenesis through Akt- transcription factor
32 EB (TFEB) axis. TFEB is a master regulator of lysosomal biogenesis and autophagy, and SopB
33 restricts the nuclear localization of TFEB. This reduces the overall lysosome content inside
34 host macrophages, further facilitating survival in macrophages and systemic dissemination of
35 *Salmonella* in the host.

36

37 Keywords: *Salmonella*-containing vacuoles, macrophages, autophagy, phosphatidylinositol,
38 TFEB, lysosomal biogenesis.

39

40 Introduction:

41 *Salmonella enterica* causes a range of infections, from self-limiting gastroenteritis to systemic
42 typhoid fever in humans (Majowicz, Musto et al. 2010). *Salmonella* can gain access to non-
43 phagocytic host cells through type 3 secretion system (T3SS) encoded by *Salmonella*
44 pathogenicity island-1 (SPI-1) (Galan and Curtiss 1989, Collazo and Galan 1997) or directly
45 phagocytosed by immune cells. Upon entering into the host cell, *Salmonella* resides in a unique
46 membrane-bound compartment called *Salmonella*-containing vacuoles (SCVs)(Eswarappa,
47 Negi et al. 2010, LaRock, Chaudhary et al. 2015). The stealthy pathogen injects several effector
48 proteins by another T3SS encoded by SPI-2 to subvert the host innate defense pathways.
49 Macrophages are the first line of host-innate immune cells that evade pathogen encounter.
50 However, in the case of *Salmonella* Typhimurium pathogenesis, it is evident that the pathogen
51 escapes the killing by macrophages and establish a replicative niche inside the cells to facilitate
52 the systemic disease in susceptible hosts (Fields, Swanson et al. 1986, Leung and Finlay 1991,
53 Das, Lahiri et al. 2009). Intracellularly, SCVs mature sequentially from the early (near
54 periphery) to late SCVs (near juxtanuclear position) (LaRock, Chaudhary et al. 2015). In
55 contrast, 10-20% of the SCV in epithelial cells rupture the vacuolar membrane and are either
56 targeted to autophagic machinery or escape killing followed by hyper-proliferation (Perrin,
57 Jiang et al. 2004, Malik-Kale, Winfree et al. 2012, Knodler, Nair et al. 2014). The cytosolic
58 bacteria inside the macrophages encounter higher levels of stress such as high reactive oxygen
59 species (ROS), reactive nitrogen species (RNS), antimicrobial peptides, metal
60 starvation/toxicity, TLR/NLR signaling and a robust xenophagic machinery (Birmingham,
61 Smith et al. 2006, Lahiri, Das et al. 2008, Das, Lahiri et al. 2009, Gogoi, Shreenivas et al.
62 2019). Therefore, bacteria must maintain the intact vacuolar membrane when residing inside
63 the macrophages.

64 Several studies have shown that the *Salmonella* in SCV can escape autophagic machinery and
65 proliferate inside hostile host cells when the vacuolar integrity is maintained. The autophagic
66 adaptors, LC3B, SQSTM/p62, and NDP52 target cytosolic bacterium (Birmingham and
67 Brumell 2006, Cemma, Kim et al. 2011), and Galectin-8 marks the damaged SCV membranes
68 and then cleared through autophagy (Thurston, Wandel et al. 2012). Interestingly, the
69 mechanisms are not clear yet how the intact SCV escapes the recruitment of autophagic
70 machinery/adaptors and avoids fusion with the terminal lysosomes.

71 The fusion of autophagosomes with lysosomes majorly depends on the phosphoinositides
72 regulation/conversion. The role of especially phosphatidylinositol 3-phosphate (PI(3)P) has
73 been well characterized in autophagosome formation. In yeast, the dephosphorylation of PI(3)P
74 by PI(3)P phosphatase, Ymr1, is an important event during the fusion of autophagosomes with
75 the lysosomes (Cebollero, van der Vaart et al. 2012). The conversion of PI(3)P initiates the
76 dissociation of the ATG machinery from the autophagosomal membranes leading to fusion
77 with the terminal lysosomes. *Salmonella* also inhibits the fusion of SCVs with the lysosomes
78 and autophagosomes when the vacuolar integrity is maintained. One of the effector molecules
79 secreted by SPI-1, SopB, is known to act as phosphatidylinositol phosphatase, which converts
80 PI(4,5)P to PI(3)P (Terebiznik, Vieira et al. 2002, Hernandez, Hueffer et al. 2004, Mason,
81 Mallo et al. 2007, Mallo, Espina et al. 2008). Therefore, we hypothesized that SopB could be
82 a potential candidate that inhibits the fusion of SCV with autophagosomes.

83 It is also well studied that SopB, even though a phosphatase, can activate Akt/protein kinase B
84 by phosphorylating Ser473 residue and thus modulate downstream signaling in infected cells.
85 SopB also inhibits apoptosis in the infected cells by activating Akt (Steele-Mortimer, Knodler
86 et al. 2000, Knodler, Finlay et al. 2005, Raffatellu, Wilson et al. 2005). On the other hand, Akt
87 is one of the critical modulators of Transcription Factor EB (TFEB) by phosphorylating TFEB
88 at Ser467 residue. The phosphorylated TFEB (Ser467) shows reduced nuclear localization,

89 resulting in downregulation of the genes under the TFEB promoter(Palmieri, Pal et al. 2017).
90 TFEB positively regulates the set of genes under its promoter, termed as Coordinated
91 Lysosomal Expression and Regulation (CLEAR) network in addition to autophagy
92 genes(Settembre, Di Malta et al. 2011).

93 Interestingly, a previous study from our lab demonstrated that the number of lysosomes inside
94 infected cells decreases upon *Salmonella* infection progression (Eswarappa, Negi et al. 2010).
95 However, the mechanism as to how *Salmonella* depletes the number of lysosomes upon
96 infection is unknown. Therefore, we hypothesized that SopB might play a dual role in
97 subverting autophagy by (1) avoiding fusion with autophagosomes or lysosomes and (2)
98 downregulating the overall lysosomes biogenesis by restricting transcription factor localization
99 to the nucleus in the infected cells.

100 We show that *Salmonella* SopB employs dual mechanisms to modulate xenophagy. The first
101 one is by accumulating PI(3)P on the SCV membranes, which successfully inhibits recruitment
102 of autophagic adaptors on the SCV and the fusion of intact SCV with auto-
103 phagolysosomes/lysosomes. The second mechanism employed by SopB is to restrict nuclear
104 localization of TFEB, leading to downregulation of overall biogenesis of lysosomes and
105 autophagosomes in macrophages. This gives the pathogen an advantage of survival as the ratio
106 of SCV to lysosomes reduces. Thus, showing novel mechanisms that *Salmonella* Typhimurium
107 SopB employs in subverting innate cellular defenses of the host that can serve as potential
108 intervention targets.

109

110 **Results:**

111 **The intracellular proliferation of STM $\Delta sopB$ is attenuated in macrophages due to the**
112 **recruitment of autophagic SNARE STX17**

113 *Salmonella* SopB is one of the key effector proteins secreted by SPI-1 machinery into the host
114 cell, and its role in inducing the uptake of the bacterium by epithelial cells has been well
115 established (Raffatellu, Wilson et al. 2005). However, the role of SopB in the macrophages has
116 not been fully elucidated. Therefore, we explored whether SopB has any role in phagocytosis
117 and intracellular proliferation in macrophages. We found that in murine macrophage cell line
118 RAW264.7, the STM $\Delta sopB$ mutant (knockout) had attenuated proliferation compared to
119 *Salmonella* Typhimurium wildtype (STM WT) or STM $\Delta sopB:sopB$ (complemented strain).
120 However, the percentage of phagocytosis remains unaltered compared to WT (**Figure 1A**). The
121 attenuated proliferation of STM $\Delta sopB$ mutant was also valid for human macrophage cell lines
122 such as PMA stimulated U937 (**Figure 1B**) and Thp1 (**Figure 1D**) and mouse primary
123 peritoneal macrophages (**Figure 1C**) as well. None of the strains exhibited any growth
124 difference in *in-vitro* Luria Bertani (LB) broth (Figure S1A). Studies have shown that SopB is
125 essential for the entry of *Salmonella* into the non-phagocytic host cells (Hume, Singh et al.
126 2017).

127 Our data corroborated with Stévenin et al., that STM $\Delta sopB$ mutant maintains vacuolar
128 integrity inside macrophages (**Figure S1N**) (Stévenin, Chang et al. 2019). This eliminates the
129 possibility of encountering with high amount of reactive oxygen species, reactive nitrogen
130 species and cationic antimicrobial peptides (Gogoi, Shreenivas et al. 2019). Therefore, we
131 further analyzed the recruitment of autophagic markers onto the SCV membranes. One of the
132 critical autophagic SNARE proteins is Syntaxin 17 (STX17), which mediates the fusion of
133 autophagosomes with lysosomes (Nakamura and Yoshimori 2017). At 2 hours post-infection

134 (2 hpi), we observed that the colocalization of STX17 onto the SCV membrane was comparable
135 to STM WT and STM $\Delta sopB$ mutants. However, at later time points (10 hpi), there was a
136 significant reduction of STX17 recruitment onto SCV membrane of STM WT and increased
137 recruitment of STX17 onto SCV of STM $\Delta sopB$ mutants (**Figure 1E- G**). This phenotype was
138 rescued in complemented strain (**Figure S1B- E**). We also have observed similar results in the
139 case of human macrophages (U937) and mouse primary peritoneal macrophages upon infection
140 with STM WT and STM $\Delta sopB$ mutants (**Figure S1G-K**).

141 These observations indicate that SopB possibly inhibits the recruitment of autophagy
142 machinery (STX17) onto the SCV membrane in macrophages. So, to further delve into the role
143 of STX17, we carried out an intracellular fold proliferation assay of *Salmonella* in STX17
144 knockdown macrophages. We found that in the STX17 knockdown condition, the STM WT
145 and STM $\Delta sopB$ mutants were able to survive significantly better than the scrambled control
146 (**Figure 1I**). We also observed that the mean fluorescence intensity (MFI) of STX17 as
147 visualized by confocal microscope was significantly lesser in the case of STM WT infection
148 than STM $\Delta sopB$ mutant infection (**Figure 1F, S1E**). Therefore, we analyzed the transcript
149 levels of STX17 in infected RAW264.7 macrophages at different time points. We observed
150 downregulation of STX17 transcript in the case of STM WT and STM $\Delta sopB:sopB$
151 (complemented strain) with the progression of infection but not in STM $\Delta sopB$ mutant infected
152 macrophages. Interestingly, we did not observe any changes in the transcript levels of STX17
153 cognate SNAREs (**Figure S2A- C**). These results indicated unknown underlying mechanisms
154 might be employed by *Salmonella* SopB, which enables it to downregulate an autophagic
155 SNARE at transcript levels.

156 **SopB inhibits the recruitment of other autophagic markers onto the SCV membrane**

157 Next, we investigated whether the SopB plays a role in recruiting other autophagy adaptors
158 such as LC3B and p62/SQSTM onto SCV, which are known autophagy adaptors, especially
159 targeting intracellular pathogens(Wang, Yan et al. 2018). We found that similar to STX17,
160 SopB also inhibits recruitment of both LC3B and p62/SQSTM onto SCV (**Figure 2A-B**) as
161 observed by the colocalization coefficient (**Figure 2C-D**). We also observed a significantly
162 lesser number of puncta of p62/SQSTM per cell in STM WT infected macrophage cells than
163 STM Δ sopB (Figure 2E), suggesting the overall induction of autophagy is significantly lesser
164 in STM WT infected RAW264.7 macrophage cells. We also observed that recruitment of LC3B
165 was pronounced in PFA treated STM WT (dead bacteria control) and in non-pathogenic *E. coli*
166 DH5 α (**Figure S2D**). These observations strongly suggested that SopB is involved in
167 restricting the induction of autophagy and inhibiting the recruitment of autophagy adaptor
168 molecules on SCV in macrophages. We also observed a significant downregulation of adaptor
169 proteins such as NDP52, LC3B, and p62/SQSTM in STM WT infected macrophages compared
170 to STM Δ sopB. Therefore, we next sought to assess the protein levels of these adaptor
171 molecules, and we found that most of them were upregulated in the case of STM Δ sopB mutants
172 (**Figure 2I, S3A**), suggesting a possible role of SopB in mediating the downregulation of
173 autophagy adaptor proteins inside infected macrophages.

174 **SopB inhibits fusion with autophagosomes and lysosomes by altering the**
175 **phosphoinositide dynamics.**

176 SopB being a phosphoinositide phosphatase, is well known to alter the PI(3)P levels of SCV.
177 Bakowski and colleagues had shown previously that the SopB is a crucial effector molecule
178 that inhibits the fusion of SCV with lysosomes(Bakowski, Braun et al. 2010). Therefore, we
179 hypothesized that similar mechanisms might help SCV avoid fusion with
180 autophagosomes/auto-phago-lysosomes. We observed that the fusion events of SCV with
181 autophagosome or lysosomes are reduced in STM WT infected macrophages compared to the

182 STM $\Delta sopB$ mutants (**Figure 3A-B**). This finding corroborated with the previous finding and
183 provided newer insight that SopB plays a crucial role in dampening the fusion of SCV with
184 autophagosomes.

185 Interestingly, the overall fluorescence intensity and puncta of LC3B are also reduced in STM
186 WT infected cells compared to STM $\Delta sopB$. Next, we isolated the SCV from infected
187 macrophages and performed mass ELISA, and we found significantly higher PI(3)P levels in
188 STM WT isolated SCVs, which was completely abrogated in STM $\Delta sopB$ mutant SCVs.
189 Concomitantly, the levels of PI4P onto the STM $\Delta sopB$ mutant SCV were significantly higher
190 with the progression of infection (**Figure 3G-H**). We also investigated the overall levels of
191 PI(3)P and PI(4)P in the infected macrophages, and we observed that the levels of PI(3)P were
192 overall higher in the case of STM WT infected cells than STM $\Delta sopB$ mutant. The levels of
193 PI4P were only higher in cells infected with STM $\Delta sopB$ mutant at 10h post-infection (**Figure**
194 **S3B-C**). We further performed Texas red Ovalbumin (TROV) chase experiments with a
195 catalytically dead SopB mutant (C460S) (**Figure S3E**) and the STM $\Delta sopB$ mutants to confirm
196 our findings. In line with our previous observation, we find that SopB is a crucial effector
197 inhibiting the fusion of SCV with autophagosomes and lysosomes (**Figure 3I-J**). Together, all
198 these data indicated that SopB is a key effector molecule from *S. Typhimurium* that helps
199 inhibit the fusion of SCV with lysosomes and autophagosomes.

200 **SopB downregulates the overall lysosomal biogenesis by restricting the nuclear
201 localization of TFEB into the nucleus.**

202 Since SopB is also a known Akt or Protein Kinase B modulator, it is involved in
203 phosphorylation of Akt at Ser473 residue (Steele-Mortimer, Knodler et al. 2000, Knodler,
204 Finlay et al. 2005, Raffatellu, Wilson et al. 2005). Interestingly, it is known that Akt can
205 phosphorylate TFEB at Ser467 residue. The phosphorylated TFEB (Ser467) shows reduced

206 nuclear localization, resulting in downregulation of the genes under the TFEB promoter
207 (Palmieri, Pal et al. 2017). TFEB upregulates the set of genes under its promoter, termed as
208 Coordinated Lysosomal Expression and Regulation (CLEAR) network and autophagy
209 genes (Settembre, Di Malta et al. 2011). These genes are responsible for lysosomal biogenesis
210 and autophagy-related processes under physiological conditions. We observed that upon
211 infection with STM WT, there is an overall downregulation of the set of genes under TFEB
212 (**Figure 4A-G**). This was further confirmed in another human cell line- U937 as well. We have
213 also confirmed the same with confocal microscopy, where we observed that the TFEB nuclear
214 localization was reduced in the case of STM WT as compared to catalytically dead mutant or
215 STM Δ sopB mutants where we observed an increased colocalization of TFEB into the nucleus
216 similar to a non-pathogenic *E. coli* DH5 α (**Figure 4H-K**).

217 We were then interested in deciphering if the same phenomena occur in the animal model
218 system; we observed that the overall bacterial burden in organs was less in STM Δ sopB mutants
219 than WT or complemented strain. So, we further assess the levels of the genes under TFEB
220 promoter in different tissues colonized by *Salmonella* of the infected mice. We observed that
221 SopB is involved in the overall downregulation of these genes at a tissue level, reducing the
222 overall lysosomal biogenesis and autophagy flux in tissue-specific levels (**Figure 4L-O**).
223 Together, these results suggest that SopB inhibits overall lysosomal biogenesis and autophagic
224 pathways through the TFEB-Akt axis. Our study reveals dual mechanisms employed by SopB
225 to subvert host-mediated xenophagy in macrophages.

226

227

228 **Discussion:**

229 Facultative and obligated intracellular pathogens are known to modulate the host endocytic
230 pathways to establish their unique replicative niche in host cells. Several bacterial molecules
231 regulate host endocytic or defense pathways (Weber and Faris 2018). Xenophagy of the
232 bacterium is one of the crucial pathways employed by host cells to keep the bacteria infection
233 in check (Wileman 2013). *Coxiella burnetii* utilizes autophagosomes that provide the bacteria
234 with a source of the membrane, facilitating its survival within host cells (Romano, Gutierrez et
235 al. 2007, Vazquez and Colombo 2010). However, in the case of *Legionella pneumophila*, which
236 subverts autophagy and cross-talk between ER-mitochondria by cleaving the syntaxin 17 with
237 effector molecule Lpg1137 (Arasaki, Mikami et al. 2017). Therefore, establishing a successful
238 niche inside the host cell is pathogen-specific.

239 *Salmonella* proliferates within-host innate immune cells like macrophages and utilizes the
240 niche to establish systemic infection (Fields, Swanson et al. 1986, Leung and Finlay 1991, Das,
241 Lahiri et al. 2009). Even though studies have shown more significant participation of SPI-2
242 effectors in intracellular survival and proliferation, well-orchestrated cross-talk between SPI-1
243 and SPI-2 effectors cannot be undermined (Lou, Zhang et al. 2019). Several diverse canonical
244 roles of SopB (SPI-1 effector) are well dissected in epithelial cells, where studies show that
245 SopB is associated with facilitating hyper-replication once the bacterium is in the cytosol of
246 epithelial cells. However, there is a dearth in understanding the role of SopB in macrophages.
247 Macrophages are professional phagocytes that can take up bacteria without induction and
248 mounts more robust xenophagy than epithelial cells (Germic, Frangez et al. 2019), indicating
249 that *Salmonella* might subvert or utilize host xenophagy depending on the cell type it is
250 residing.

251 We report a model (Figure 4) for the first time that, SopB subverts xenophagy in host
252 macrophages through a dual mechanism. Firstly, it alters the PI(3)P levels of the SCV
253 membrane to inhibit its fusion with auto-phagolysosomes and lysosomes. Intracellular
254 pathogens often find their haven inside the modified phagosome or vacuolar environment of
255 host cells to remain hidden from innate defense pathways. Whence there is a possibility that
256 due to altered PI(3)P levels, SCV remains as a hidden organelle inside the host cells. Thus,
257 autophagy machinery fails to identify it, resulting in escaping an otherwise robust innate
258 defense mechanism.

259 Our lab and others have shown that intracellular pathogens modulate the lysosomal biogenesis
260 in host cells(Sachdeva and Sundaramurthy 2020). We here report a second mechanism
261 employed by SopB to downregulate the overall lysosomal and autophagosomal biogenesis
262 through the TFEB-Akt axis, reducing overall lysosomal content in infected macrophages,
263 thereby giving an upper hand to an intracellular pathogen because of the number of active
264 lysosomal to SCV ratio reduces. Our study also draws attention towards therapeutic strategies
265 that can be further delved into to assess the ability of small molecule inhibitors (against SopB)
266 or activators of TFEB, which might help reduce systemic *Salmonella* infection through
267 macrophages.

268 **Material and Methods**

269 **Bacterial strains and growth condition**

270 *Salmonella enterica* serovars Typhimurium (STM) wild type strain ATCC SL13344, STM
271 *ΔsopB*, STM *ΔsopB*: *sopB* (expressing SopB through a pWSK29-low copy number plasmid)
272 were a kind gift from Prof. Michael Hensel, Abteilung Mikrobiologie, Universität Osnabrück,
273 Osnabrück, Germany. *E. coli* DH5 α were cultured in Luria broth (LB-Hi-media) with constant
274 shaking (175rpm) at 37°C. Ampicillin or kanamycin was used wherever required. The bacteria

275 were tagged with mCherry with pPFPV 25.1 plasmids for immunofluorescence studies. Site-
276 directed mutagenesis was done by Phusion polymerase (New England Bio Labs) using a primer
277 as previously described(Liebl, Qi et al. 2017) to generate STM $\Delta sopB$: C460S *sopB* (expressing
278 C460S SopB through a pWSK29-low copy number plasmid).

279 **Cell culture protocol**

280 The cells RAW264.7 murine macrophages were cultured in DMEM - Dulbecco's Modified
281 Eagle Medium (Sigma) supplemented with 10% FBS (Gibco) at 37°C in a humidified incubator
282 (Panasonic) with 5% CO₂. Prior to each experiment, the cells were seeded onto the required
283 plate either with a coverslip (for confocal fluorescence microscopy) or without (for intracellular
284 survival assay, qRT-PCR and western blotting) at a confluence of 80-90%.

285 Human monocytes/macrophages U937 and Thp1 were cultured in RPMI- Roswell Park
286 Memorial Institute media supplemented with 10% FBS (Gibco) at 37°C in a humidified
287 incubator (Panasonic) with 5% CO₂. Prior to each experiment, the cells were seeded with
288 Phorbol-12-myristate-13-acetate (PMA- Sigma) at a concentration of 20ng/mL onto the
289 required plate either with a coverslip (for confocal fluorescence microscopy) or without (for
290 intracellular survival assay, qRT-PCR and western blotting) at a confluence of 80-90%.

291 Peritoneal macrophages isolation was performed as previously described (Zhang, Goncalves et
292 al. 2008). Briefly, 4-6 weeks C57BL/6 mice were injected with Brewer's thioglycollate media
293 (Hi-Media) in the peritoneal cavity, and after 4-5 days post-intra-peritoneal (i.p.) injection, the
294 cells were harvested from the peritoneal cavity. Cells were then seeded, and 24hour post-
295 harvesting experiments were performed.

296 **Gentamicin protection assay**

297 The cells were then infected with *Salmonella* Typhimurium (STM) (strain SL1344), STM
298 $\Delta sopB$, STM $\Delta sopB$: *sopB*, STM WT PFA fixed and DH5 α . at MOI of 25 for confocal

299 experiment. Upon infecting the RAW264.7 cell-line, the plate was centrifuged at 700-900 rpm
300 for 5 mins to facilitate the adhesion and then incubated for 20mins at 37°C and 5% CO₂. Post-
301 incubation, the bacteria containing media were removed, and wells were twice washed with
302 PBS, and fresh media was added containing 100µg/mL gentamicin, incubated for 1 hour at
303 37°C and 5% CO₂. Following this, the media was removed, washed with PBS twice and
304 25µg/mL gentamicin-containing media was added and incubated for different time points at
305 37°C and 5% CO₂. Time points selected for confocal microscopy, qRT-PCR and immuno-
306 blotting were 2 hours, 6 hours and 10 hours post-infection. The time points were 2 hours and
307 10 hours for intracellular survival assay.

308 **Confocal Microscopy**

309 After appropriate hours of incubation post-infection with STM-WT, STM *ΔsopB*, STM *ΔsopB*:
310 *sopB*, STM WT PFA fixed and DH5 α . The cells on coverslips were washed thrice with PBS
311 and fixed with 3.5 % paraformaldehyde for 10-15mins. Then cells were washed twice with PBS
312 and incubated with a specific antibody (α - STX 17 (Protein-Tech) or α - LC3B(Novus
313 Biologicals) in a blocking buffer containing 2 % BSA and 0.01% saponin for 3 hours at room
314 temperature (RT) or overnight at 4°C. Following this, the cells were washed twice with PBS
315 and incubated with an appropriate secondary antibody tagged with fluorochrome for 1 hour at
316 RT. The coverslips were then mounted onto a clean glass slide with mounting media and
317 antifade agent; after the mounting media dried, it was sealed with clear nail polish and imaged
318 under a confocal scanning laser microscope (Zeiss 880 microscope, at 63X oil immersion, 2x-
319 3x zoom).

320 **Bacterial enumeration for intracellular survival assay**

321 After appropriate hours of incubation post-infection with STM- WT, the mammalian cells were
322 lysed by 0.1 % Triton-X 100. Then the lysate was plated onto *Salmonella*-Shigella (SS) Agar

323 plate at appropriate dilutions. Percentage invasion and fold proliferation were then calculated
324 with the following formula.

325 Percent invasion = CFU at 2h / CFU of Pre-Inoculum * 100

326 Fold Proliferation = CFU at 10h/ CFU at 2h.

327 **RNA isolation and quantitative RT PCR**

328 RNA isolation was performed from transfected cells after appropriate hours of infection with
329 STM WT at MOI of 10 or from tissue samples mesenteric lymph nodes (MLN), spleen and
330 intestine (infected C57BL/6) by using TRIzol (Takara) reagent according to manufacturers'
331 protocol. Quantification of the RNA was done in NanoDrop (Thermo-Fisher Scientific). To
332 check for RNA quality, the isolated RNA was also run on 2% agarose gel, and 3µg of RNA has
333 subjected to DNase 1 treatment at 37°C. The reaction was then stopped with the addition of
334 EDTA, and heated at 65°C for 10mins. As per the manufacturer's protocol, the cDNA was
335 synthesized by a cDNA synthesis kit (Takara). Quantitative real-time PCR was done using
336 SYBR/ TB green (TAKARA) RT-PCR kit in BioRad qRT-PCR system. The reaction was set
337 up in a 384 well plate with three replicates for each sample. The expression levels of the gene
338 of interest were measured using specific RT primers (Table S1). Gene expression levels were
339 normalized to beta-actin as an internal control.

340 **Transient Transfection**

341 RAW 264.7 cells were seeded at a 50-60% confluence 12 hours prior to transfecting using
342 either PEI (1:2 -DNA: PEI) or Lipofectamine 3000 (Thermo-fisher) as per manufacturer's
343 protocol. Approximately 300-500ng of plasmid DNA/well (ratio 260/280 ~1.8- 1.9) was used
344 for transfection in 24well plate, and 1-2µg of plasmid DNA/well was used for 6well plates. List
345 of plasmids used is given in Table S2. Cells were then incubated for 8hours at 37°C in a
346 humidified incubator with 5% CO2; after that, the media containing transfecting DNA and

347 reagents were removed, and cells were further incubated for 48 hours in complete media
348 DMEM +10% FBS. Cells were then either harvested for further analysis or infected with the
349 required MOI.

350 **Isolation of *Salmonella* containing vacuole (SCV) by Ultracentrifugation**

351 The isolation of SCV was performed as previously described (Luhrmann and Haas 2000).
352 Roughly 50 million RAW264.7 cells infected with *S. Typhimurium* SL1344 strain were used
353 for subcellular fractionation of SCVs. At 2 hr, 6 hr and 10 hr p.i., cells were washed thrice with
354 ice-cold PBS and scrapped into a 15 ml centrifuge tube using a rubber cell scraper. The cells
355 were centrifuged at 1000 rpm for 7 min, and the cell pellets were suspended in ice-cold
356 homogenization buffer (250 mM sucrose, 20 mM HEPES (pH 7.2), 0.5 mM EGTA and protease
357 inhibitor cocktail (Roche) and transferred to a Dounce Homogenizer with a tight-fitting pestle
358 on ice to break the cells. Approximately 30 strokes were applied until almost 90% of the cells
359 were broken without breaking the nuclei. The intact cells and nuclei were pelleted at 400 x g
360 for 3 min. The resulting supernatant was collected in a fresh tube to yield the post-nuclear
361 supernatant (PNS). The PNS was brought to a final concentration of 39% sucrose and layered
362 on to 2 ml 55% sucrose, which was layered onto a 65% sucrose cushion in a 13.2 ml open-top
363 Beckman ultracentrifuge tube followed by the addition of 2 ml 32.5% and 2 ml 10% sucrose
364 solutions. All sucrose solutions (w/v) were prepared in 20 mM HEPES (pH 7.2) and 0.5 mM
365 EGTA. The PNS layered on sucrose gradient was then subjected for ultracentrifugation in a
366 swinging bucket rotor for 1 hr at 100000 x g at 4°C. The fractions of 1 ml each were collected
367 from top to bottom. Pooled fractions 8-10 were adjusted very slowly to a final sucrose
368 concentration of 11% with homogenization buffer without sucrose and layered on a 15% Ficoll
369 cushion (5% sucrose, 0.5 mM EGTA and 20 mM HEPES pH 7.2). The samples in an open-top
370 Beckman ultracentrifuge tube were spun at 18000 x g for 30 minutes in a Beckman SW 41 Ti
371 rotor at 4°C. The supernatant was discarded, and the pellet was resuspended in an 11 ml

372 homogenization buffer. The samples were spun again at 18000 x g for 20 min in a Beckman
373 SW 41 Ti rotor at 4°C, and the resulting pellet was labelled as an “SCV” fraction. The pelleted
374 SCV fractions were resuspended in 200µL of homogenization buffer.

375 **PI(3)P and PI(4)P Mass ELISA:**

376 Isolated SCV fraction from infected RAW264.7 macrophages were further processed for lipid
377 isolation and the isolated lipids were quantified using PI(3)P and PI(4)P mass ELISA kits
378 (Echelon Biosciences) as per manufacturer’s protocol.

379 **Texas Red Ovalbumin Pulse chase experiment:**

380 RAW 264.7 cells were seeded at a 50-60% confluence 12 hours prior to treatment with Texas
381 red Ovalbumin (Thermo-Fischer Scientific) at a concentration of 50µg/mL for 30minutes at
382 37°C in a humidified incubator with 5% CO₂. Next, media was removed and fresh medium
383 with stationary phase bacteria (10-12hours old) at a MOI of 25 was added to the cells and further
384 incubated for 25mins in humidified incubator. At indicated timepoints cells were washed twice
385 with 1X PBS and fixed with 3.5% paraformaldehyde for 15minutes. Cells were images under
386 microscope after staining with anti-*Salmonella* antibody (Zeiss LSM 880) using 63X oil
387 immersion objective lens and images were analysed with ZEN Black 2009 software by Zeiss.

388 **In-vivo experiments**

389 6 weeks old C57BL/6 mice were infected by oral gavaging of 10⁷ CFU of STM WT, STM
390 *ΔsopB*, or STM *ΔsopB: sopB*. 5 days post-infection, mice were sacrificed, and organs such as
391 the liver, spleen, MLN, brain and intestine were plated onto SS agar, and tissue samples from
392 spleen MLN and intestine were also used for RNA isolation and further analysis.

393 **Immunoblotting**

394 After appropriate hours of infection with STM WT at MOI of 10, the media was removed, and
395 the cells were washed twice with PBS. Cells were then harvested using a sterile scraper and
396 centrifuged at 1500 rpm for 10 mins, 4°C. Cell lysis was done by RIPA buffer for 30mins on
397 ice, followed by estimation of total protein using Bradford protein estimation method.
398 Polyacrylamide Gel Electrophoresis (PAGE) was done by loading 35 μ g of protein from whole
399 cell lysate, then transferring onto 0.45 μ m PVDF membrane (GE Healthcare). The membrane
400 was blocked using 5% skimmed milk (Hi-Media) in TTBS for 1h at RT and then probed with
401 specific primary and secondary HRP conjugated antibodies. The membrane was developed
402 using ECL (Bio-rad), and images were captured using ChemiDoc GE healthcare. All
403 densitometric analysis was performed using the Image J Platform.

404 **Statistical analysis**

405 Each experiment has been independently performed at least 3 times (as mentioned in figure
406 legends). Confocal data sets were analysed and quantified in Zen 2.3 platform by Zeiss. The
407 data sets were analysed by unpaired student's t-test by GraphPad Prism 8.4.3 software, and *p*-
408 *values* are indicated in the figures and legends for reference. The results are either expressed as
409 mean \pm SEM or mean \pm SD as indicated in the legends. Data obtained from *in-vivo* mouse
410 experiments were analysed by Mann-Whitney *U* test from GraphPad Prism 8.4.3 software

411 **Acknowledgment:**

412 Divisional and Departmental Confocal Facility, Departmental Real-Time PCR Facility, and
413 Central Animal Facility at IISc are duly acknowledged. Mr. Punith, Mrs. Saima and Ms. Navya
414 are acknowledged for their help in image acquisition. Ms. Sukeerthi, Ms. Nishi and Ms. Rhea
415 are acknowledged for their technical help.

416 **Funding:**

417 This work was supported by the Department of Biotechnology (DBT), Ministry of Science and
418 Technology, the Department of Science and Technology (DST), Ministry of Science and
419 Technology. DC acknowledges DAE-SRC ((DAE00195) outstanding investigator award and
420 funds and ASTRA Chair Professorship funds. The authors jointly acknowledge the DBT-IISc
421 partnership program. Infrastructure support from ICMR (Center for Advanced Study in
422 Molecular Medicine), DST (FIST), UGC-CAS (special assistance), and TATA fellowship is
423 acknowledged. This work was also supported by the Department of Biotechnology
424 (BT/PR32489/BRB/10/1786/2019), Science and Engineering Research Board
425 (CRG/2019/000281), DBT-NBACD (BT/HRD-NBA-NWB/38/2019-20) and India Alliance
426 (500122/Z/09/Z) to SRGS. RC duly acknowledges CSIR-SRF fellowship.

427 **Availability of data and materials**

428 All data generated and analysed during this study, including the supplementary information
429 files, have been incorporated in this article. The data is available from the corresponding author
430 on request.

431 **Declarations**

432 **Ethics statement**

433 All the animal experiments were approved by the Institutional Animal Ethics Committee, and
434 the Guidelines provided by National Animal Care were strictly followed. (Registration No:
435 48/1999/CPCSEA)

436

437

438 **References:**

439 Arasaki, K., Y. Mikami, S. R. Shames, H. Inoue, Y. Wakana and M. Tagaya (2017).
440 "Legionella effector Lpg1137 shuts down ER-mitochondria communication through cleavage
441 of syntaxin 17." Nat Commun **8**: 15406.
442 Bakowski, M. A., V. Braun, G. Y. Lam, T. Yeung, W. D. Heo, T. Meyer, B. B. Finlay, S.
443 Grinstein and J. H. Brumell (2010). "The phosphoinositide phosphatase SopB manipulates
444 membrane surface charge and trafficking of the Salmonella-containing vacuole." Cell Host
445 Microbe **7**(6): 453-462.
446 Birmingham, C. L. and J. H. Brumell (2006). "Autophagy recognizes intracellular Salmonella
447 enterica serovar Typhimurium in damaged vacuoles." Autophagy **2**(3): 156-158.
448 Birmingham, C. L., A. C. Smith, M. A. Bakowski, T. Yoshimori and J. H. Brumell (2006).
449 "Autophagy controls Salmonella infection in response to damage to the Salmonella-containing
450 vacuole." J Biol Chem **281**(16): 11374-11383.
451 Cebollero, E., A. van der Vaart, M. Zhao, E. Rieter, D. J. Klionsky, J. B. Helms and F. Reggiori
452 (2012). "Phosphatidylinositol-3-phosphate clearance plays a key role in autophagosome
453 completion." Curr Biol **22**(17): 1545-1553.
454 Cemma, M., P. K. Kim and J. H. Brumell (2011). "The ubiquitin-binding adaptor proteins
455 p62/SQSTM1 and NDP52 are recruited independently to bacteria-associated microdomains to
456 target Salmonella to the autophagy pathway." Autophagy **7**(3): 341-345.
457 Collazo, C. M. and J. E. Galan (1997). "The invasion-associated type-III protein secretion
458 system in Salmonella--a review." Gene **192**(1): 51-59.
459 Das, P., A. Lahiri, A. Lahiri and D. Chakravortty (2009). "Novel role of the nitrite transporter
460 NirC in Salmonella pathogenesis: SPI2-dependent suppression of inducible nitric oxide
461 synthase in activated macrophages." Microbiology (Reading) **155**(Pt 8): 2476-2489.

462 Eswarappa, S. M., V. D. Negi, S. Chakraborty, B. K. Chandrasekhar Sagar and D. Chakravortty
463 (2010). "Division of the Salmonella-containing vacuole and depletion of acidic lysosomes in
464 Salmonella-infected host cells are novel strategies of *Salmonella enterica* to avoid lysosomes."
465 Infect Immun **78**(1): 68-79.

466 Fields, P. I., R. V. Swanson, C. G. Haidaris and F. Heffron (1986). "Mutants of *Salmonella*
467 *typhimurium* that cannot survive within the macrophage are avirulent." Proc Natl Acad Sci U
468 S A **83**(14): 5189-5193.

469 Galan, J. E. and R. Curtiss, 3rd (1989). "Cloning and molecular characterization of genes whose
470 products allow *Salmonella typhimurium* to penetrate tissue culture cells." Proc Natl Acad Sci
471 U S A **86**(16): 6383-6387.

472 Gogoi, M., M. M. Shreenivas and D. Chakravortty (2019). "Hoodwinking the Big-Eater to
473 Prosper: The *Salmonella*-Macrophage Paradigm." J Innate Immun **11**(3): 289-299.

474 Hernandez, L. D., K. Hueffer, M. R. Wenk and J. E. Galan (2004). "Salmonella modulates
475 vesicular traffic by altering phosphoinositide metabolism." Science **304**(5678): 1805-1807.

476 Hume, P. J., V. Singh, A. C. Davidson and V. Koronakis (2017). "Swiss Army Pathogen: The
477 *Salmonella* Entry Toolkit." Front Cell Infect Microbiol **7**: 348.

478 Knodler, L. A., B. B. Finlay and O. Steele-Mortimer (2005). "The *Salmonella* effector protein
479 SopB protects epithelial cells from apoptosis by sustained activation of Akt." J Biol Chem
480 **280**(10): 9058-9064.

481 Knodler, L. A., V. Nair and O. Steele-Mortimer (2014). "Quantitative assessment of cytosolic
482 *Salmonella* in epithelial cells." PLoS One **9**(1): e84681.

483 Lahiri, A., P. Das and D. Chakravortty (2008). "The LysR-type transcriptional regulator Hrg
484 counteracts phagocyte oxidative burst and imparts survival advantage to *Salmonella enterica*
485 serovar *Typhimurium*." Microbiology (Reading) **154**(Pt 9): 2837-2846.

486 LaRock, D. L., A. Chaudhary and S. I. Miller (2015). "Salmonellae interactions with host
487 processes." Nat Rev Microbiol **13**(4): 191-205.

488 Leung, K. Y. and B. B. Finlay (1991). "Intracellular replication is essential for the virulence of
489 *Salmonella typhimurium*." Proc Natl Acad Sci U S A **88**(24): 11470-11474.

490 Lou, L., P. Zhang, R. Piao and Y. Wang (2019). "Salmonella Pathogenicity Island 1 (SPI-1)
491 and Its Complex Regulatory Network." Front Cell Infect Microbiol **9**: 270.

492 Majowicz, S. E., J. Musto, E. Scallan, F. J. Angulo, M. Kirk, S. J. O'Brien, T. F. Jones, A.
493 Fazil, R. M. Hoekstra and S. International Collaboration on Enteric Disease 'Burden of Illness
494 (2010). "The global burden of nontyphoidal *Salmonella* gastroenteritis." Clin Infect Dis **50**(6):
495 882-889.

496 Malik-Kale, P., S. Winfree and O. Steele-Mortimer (2012). "The bimodal lifestyle of
497 intracellular *Salmonella* in epithelial cells: replication in the cytosol obscures defects in
498 vacuolar replication." PLoS One **7**(6): e38732.

499 Mallo, G. V., M. Espina, A. C. Smith, M. R. Terebiznik, A. Aleman, B. B. Finlay, L. E. Rameh,
500 S. Grinstein and J. H. Brumell (2008). "SopB promotes phosphatidylinositol 3-phosphate
501 formation on *Salmonella* vacuoles by recruiting Rab5 and Vps34." J Cell Biol **182**(4): 741-
502 752.

503 Mason, D., G. V. Mallo, M. R. Terebiznik, B. Payrastre, B. B. Finlay, J. H. Brumell, L. Rameh
504 and S. Grinstein (2007). "Alteration of epithelial structure and function associated with
505 PtdIns(4,5)P2 degradation by a bacterial phosphatase." J Gen Physiol **129**(4): 267-283.

506 Nakamura, S. and T. Yoshimori (2017). "New insights into autophagosome-lysosome fusion."
507 J Cell Sci **130**(7): 1209-1216.

508 Palmieri, M., R. Pal and M. Sardiello (2017). "AKT modulates the autophagy-lysosome
509 pathway via TFEB." Cell Cycle **16**(13): 1237-1238.

510 Perrin, A. J., X. Jiang, C. L. Birmingham, N. S. So and J. H. Brumell (2004). "Recognition of
511 bacteria in the cytosol of Mammalian cells by the ubiquitin system." *Curr Biol* **14**(9): 806-811.

512 Raffatellu, M., R. P. Wilson, D. Chessa, H. Andrews-Polymenis, Q. T. Tran, S. Lawhon, S.
513 Khare, L. G. Adams and A. J. Baumler (2005). "SipA, SopA, SopB, SopD, and SopE2
514 contribute to *Salmonella enterica* serotype *typhimurium* invasion of epithelial cells." *Infect*
515 *Immun* **73**(1): 146-154.

516 Romano, P. S., M. G. Gutierrez, W. Beron, M. Rabinovitch and M. I. Colombo (2007). "The
517 autophagic pathway is actively modulated by phase II *Coxiella burnetii* to efficiently replicate
518 in the host cell." *Cell Microbiol* **9**(4): 891-909.

519 Sachdeva, K. and V. Sundaramurthy (2020). "The Interplay of Host Lysosomes and
520 Intracellular Pathogens." *Front Cell Infect Microbiol* **10**: 595502.

521 Settembre, C., C. Di Malta, V. A. Polito, M. Garcia Arencibia, F. Vetrini, S. Erdin, S. U. Erdin,
522 T. Huynh, D. Medina, P. Colella, M. Sardiello, D. C. Rubinsztein and A. Ballabio (2011).
523 "TFEB links autophagy to lysosomal biogenesis." *Science* **332**(6036): 1429-1433.

524 Steele-Mortimer, O., L. A. Knodler, S. L. Marcus, M. P. Scheid, B. Goh, C. G. Pfeifer, V.
525 Duronio and B. B. Finlay (2000). "Activation of Akt/protein kinase B in epithelial cells by the
526 *Salmonella typhimurium* effector sigD." *J Biol Chem* **275**(48): 37718-37724.

527 Stévenin, V., Y.-Y. Chang, Y. Le Toquin, M. Duchateau, Q. G. Gianetto, C. H. Luk, A. Salles,
528 V. Sohst, M. Matondo, N. Reiling and J. Enninga (2019). "Dynamic Growth and Shrinkage of
529 the *Salmonella*-Containing Vacuole Determines the Intracellular Pathogen Niche." *Cell*
530 *Reports* **29**(12): 3958-3973.e3957.

531 Terebiznik, M. R., O. V. Vieira, S. L. Marcus, A. Slade, C. M. Yip, W. S. Trimble, T. Meyer,
532 B. B. Finlay and S. Grinstein (2002). "Elimination of host cell PtdIns(4,5)P(2) by bacterial
533 SigD promotes membrane fission during invasion by *Salmonella*." *Nat Cell Biol* **4**(10): 766-
534 773.

535 Thurston, T. L., M. P. Wandel, N. von Muhlinen, A. Foeglein and F. Randow (2012). "Galectin
536 8 targets damaged vesicles for autophagy to defend cells against bacterial invasion." Nature
537 **482**(7385): 414-418.

538 Vazquez, C. L. and M. I. Colombo (2010). "Coxiella burnetii modulates Beclin 1 and Bcl-2,
539 preventing host cell apoptosis to generate a persistent bacterial infection." Cell Death Differ
540 **17**(3): 421-438.

541 Wang, L., J. Yan, H. Niu, R. Huang and S. Wu (2018). "Autophagy and Ubiquitination in
542 Salmonella Infection and the Related Inflammatory Responses." Front Cell Infect Microbiol **8**:
543 78.

544 Weber, M. M. and R. Faris (2018). "Subversion of the Endocytic and Secretory Pathways by
545 Bacterial Effector Proteins." Front Cell Dev Biol **6**: 1.

546 Wileman, T. (2013). "Autophagy as a defence against intracellular pathogens." Essays
547 Biochem **55**: 153-163.

548

549

550 **Main Figures and Legends:**

551 **Figure 1: Intracellular proliferation of STM $\Delta sopB$ is attenuated in macrophages due to**
552 **recruitment of autophagic SNARE STX17.**

553 Gentamicin protection assay performed in **(A)** murine macrophage RAW 264.7 cells with
554 either STM WT or STM $\Delta sopB$ or STM $\Delta sopB:sopB$, at 2h and 10h cells were lysed and plated
555 to count CFU/mL and then fold proliferation is ratio of 16h/2h and, percentage invasion in
556 RAW 264.7 cells was calculated 2h/pre-inoculum (p.i.)*100. Gentamicin protection assay
557 performed in **(B)** human monocyte stimulated with PMA U937 cells **(C)** primary peritoneal
558 macrophage cells **(D)** human monocyte stimulated with PMA Thp1. **(E)** Representative
559 immunofluorescence images of infected RAW264.7 macrophages (MOI of 25) at 2h and
560 10hour in confocal laser scanning microscope (CLSM); Green- bacterial strain, Red- STX17,
561 yellow -colocalization. Quantification of immunofluorescence images**(F)** Mean fluorescence
562 intensity (MFI) and **(G)** colocalization coefficient was performed using ZEN 2.3 platform. **(H)**
563 Quantitative RT-PCR to assess the levels of STX17 in infected RAW264.7 macrophages with
564 STM WT or STM $\Delta sopB$ or STM $\Delta sopB:sopB$. **(I)** Intracellular survival in STX17 knockdown
565 cells. Scale bar in microscopic images is of 10 μ m and data is representative of one experiment
566 with more than 50 cells analysed for each condition. All experiments were repeated at least
567 three times N=3. Student's unpaired t-test performed for statistical analysis, mean \pm SEM/SD
568 p<0.05, ** p<0.01, *** p<0.001.

569 **Figure 2: SopB inhibits recruitment of other autophagic markers onto the SCV**
570 **membrane and also downregulate their levels at transcript and protein levels.**

571 Representative confocal microscopy images of RAW 264.7 cells infected with STM WT or
572 STM $\Delta sopB$ and fixed at different time points, stained with **(A)** LC3B or **(B)** SQSTM/p62. **(C)**
573 Quantification of LC3B colocalization at 2h and 10h. **(D)** Quantification of SQSTM/p62

574 colocalization coefficient and (E) puncta per cells were counted. Colocalization coefficient
575 using Zen 2.3 platform. Quantitative RT-PCR of (F) NDP52, (G) LC3B and (H) p62/SQSTM,
576 performed in the RAW264.7 murine macrophages infected with STM WT (blue) or STM
577 $\Delta sopB$ (red) or STM $\Delta sopB:sopB$ (green), uninfected (purple), DMSO-vehicle control
578 (orange), rapamycin treated (black) and bafilomycin A treated (brown). (I) Representative
579 immunoblotting with Beclin1, p62 and LC3B. Scale bar in microscopic images is of 10 μ m and
580 data is representative of one experiment with more than 50 cells analysed for each condition.
581 All experiments were repeated at least three times N=3. Student's unpaired t-test performed for
582 statistical analysis, Mean \pm SEM/SD * p<0.05, ** p<0.01, *** p<0.001.

583 **Figure 3: SopB inhibits fusion with autophagosomes and lysosomes by altering the**
584 **phosphoinositide dynamics**

585 Representative images of transiently transfected RAW264.7 macrophages with pDest EGFP
586 mCherry LC3B tandem construct, further infected with STM WT or STM $\Delta sopB$ and cells
587 fixed at (A) 2h and (B) 10h and further stained with anti-*Salmonella* to mark the bacterial
588 localisation. Quantification of the colocalization of EGFP and mCherry at (C) 2h and (D) 10h
589 using Zen 2.3 platform (E) Schematic of ultracentrifugation for isolation of *Salmonella*
590 containing vacuoles (SCV); (F) Immunoblotting with *Salmonella* GroEL with isolated fraction
591 after ultracentrifugation to confirm that fraction 8-SCV fraction contains the purified bacterial
592 population from infected cells. (I) To stain the terminal lysosomes 264.7 macrophages were
593 treated with Texas red ovalbumin (OVA) for 45mins prior to infection with the STM WT or
594 STM $\Delta sopB$ or STM $\Delta sopB: C460S sopB$. (J) Quantification of the MFI using Zen 2.3
595 platform. (G) Representative PI(3)P and (H) PI(4)P mass ELISA plots of the isolated SCV
596 fractions from ultracentrifugation. Scale bar in microscopic images is of 10 μ m and data is
597 representative of one experiment with more than 50 cells analysed for each condition. All

598 experiments were repeated at least three times N=3. Student's unpaired t-test performed for
599 statistical analysis, Mean \pm SEM/SD p<0.05, ** p<0.01, *** p<0.001.

600 **Figure 4: SopB downregulates the overall lysosomal biogenesis by restricting the nuclear
601 localisation of TFEB into the nucleus.**

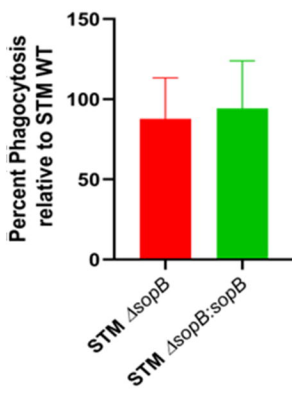
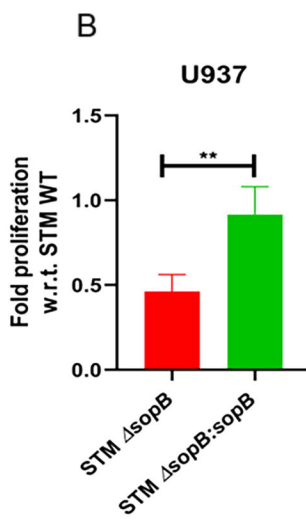
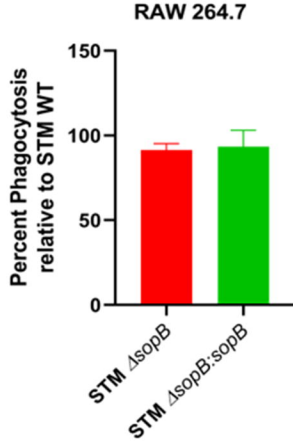
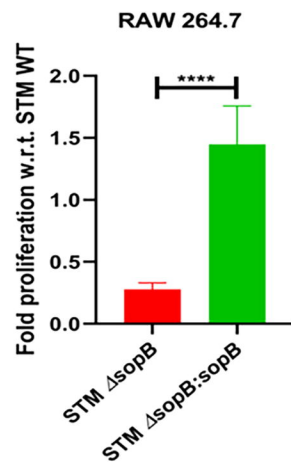
602 Representative quantitative RT-PCR for lysosomal biogenesis gene **(A)** NAGLU, **(B)**ATP6,
603 **(C)** CTSD, **(D)** GLA, **(E)** MCOLN1 **(F)** LAMP1 **(G)** CLCN7 from RAW264.7 macrophages
604 infected with STM WT or STM Δ sopB or STM Δ sopB:sopB. Representative confocal images
605 of infected RAW264.7 macrophages with mentioned bacteria in red panel and stained with
606 anti-TFEB (Green) antibody to assess its localisation inside the cells. To mark the nucleus, we
607 have used Hoechst staining RAW264.7 murine macrophages infected with **(H)** STM WT **(I)**
608 STM Δ sopB **and (N)** STM Δ sopB:sopB RAW264.7 murine macrophages, 10h post infection
609 with infection with a catalytically dead SopB harbouring STM. Scale bar in microscopic
610 images is of 10 μ m and data is representative of one experiment with more than 50 cells
611 analysed for each condition. All experiments were repeated at least three times N=3. Student's
612 unpaired t-test performed for statistical analysis, Mean \pm SEM/SD * p<0.05, ** p<0.01, ***
613 p<0.001. C57BL/6 mice of 4-6 weeks were gavaged with 10⁷ CFU/mL of bacteria and 3 days
614 post infection, mice were sacrificed **(L)** organ bacterial burden was calculated and the organs
615 tissue RNA isolated for quantitative RT-PCR in **(M)** Intestine **(N)** Spleen **(O)** MLN. All
616 quantitative RT-PCR data are representative of one biological replicate, and mean \pm SD *
617 p<0.01, ** p<0.001, *** p<0.0001.

618

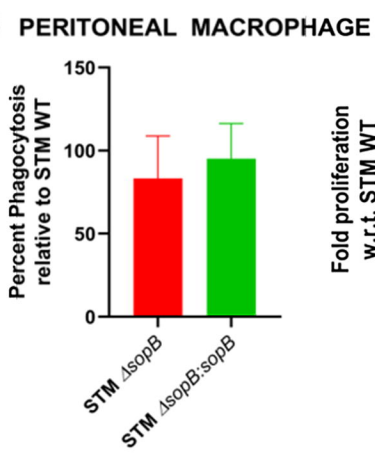
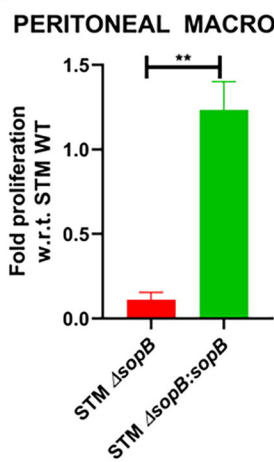
619

620

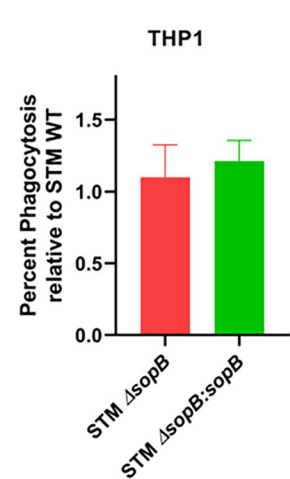
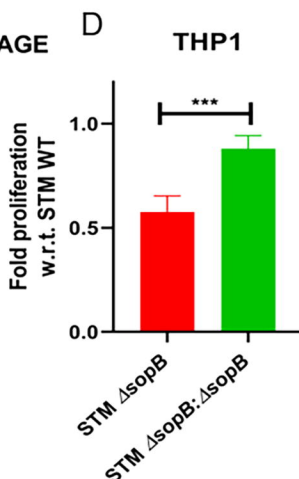
A FIGURE 1



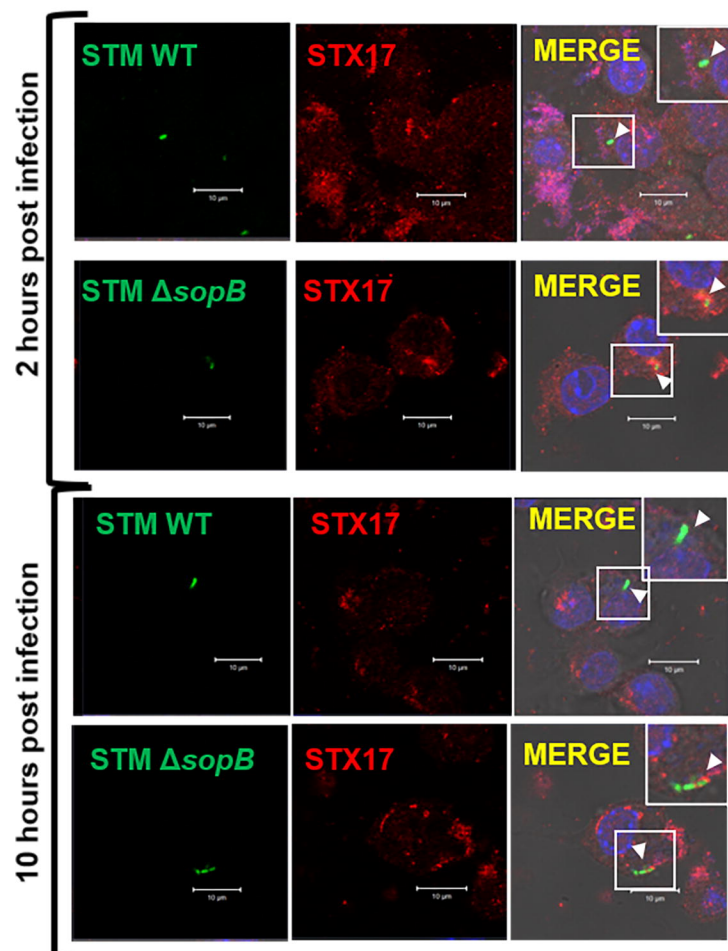
C



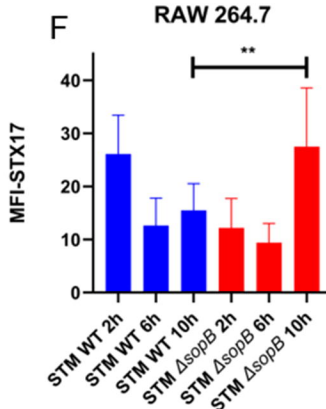
D



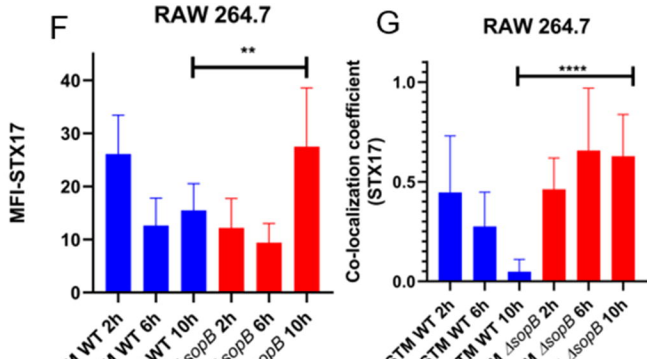
E



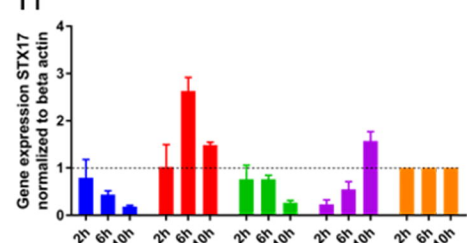
F



G



H



I

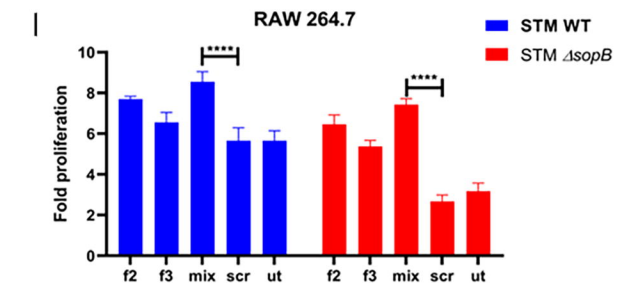
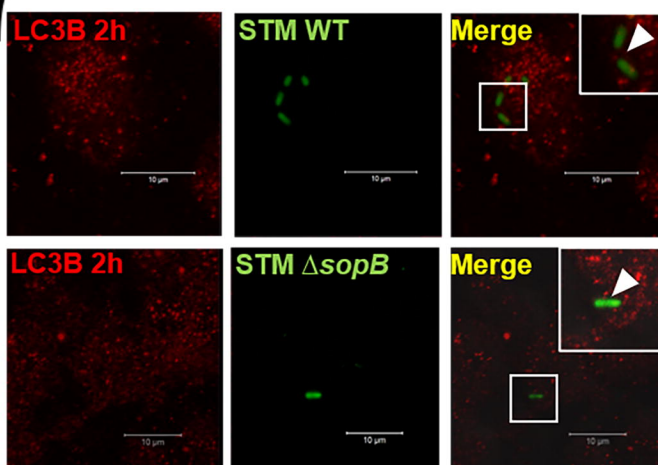
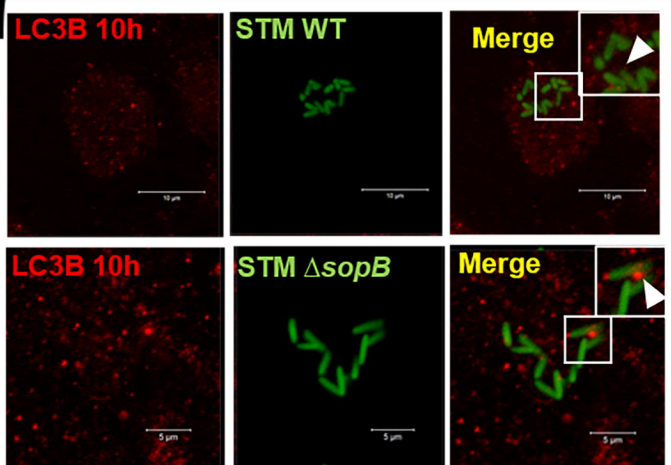


FIGURE 2

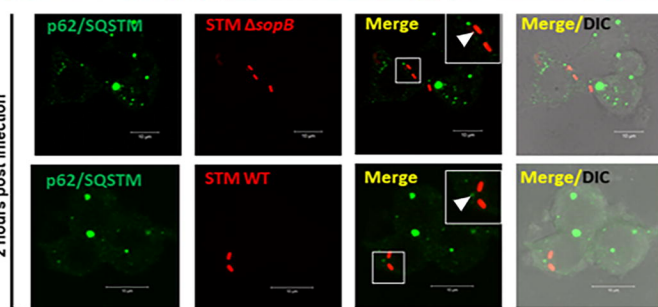
2 hours post infection



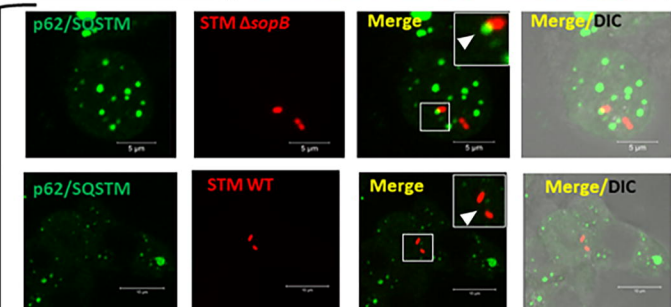
10 hours post infection



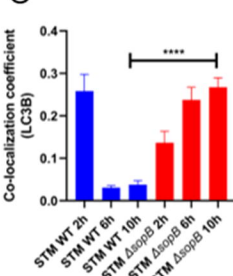
B



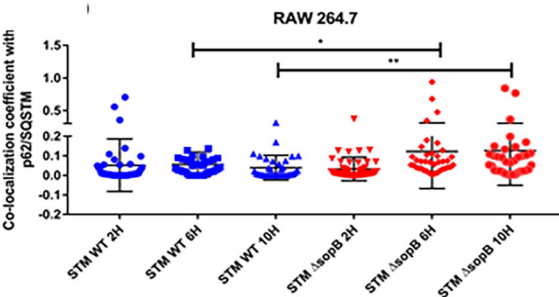
10 hours post infection



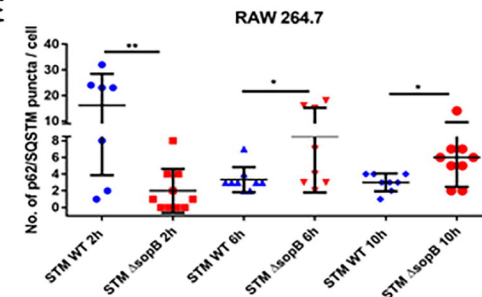
C



Co-localization coefficient with p62/SQSTM

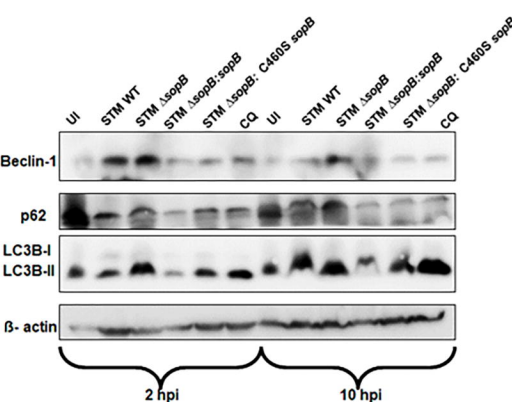
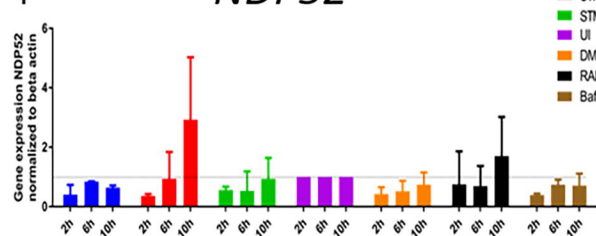


No. of p62/SQSTM puncta / cell



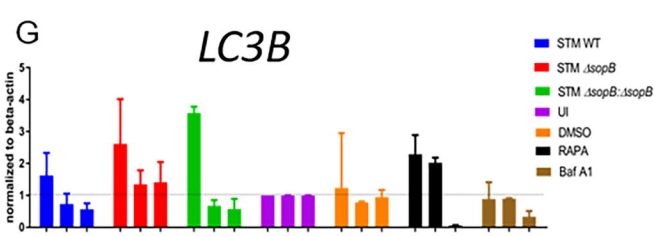
F

NDP52



G

LC3B



H

p62/SQSTM

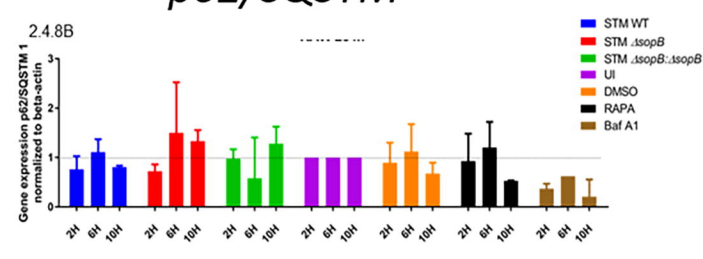
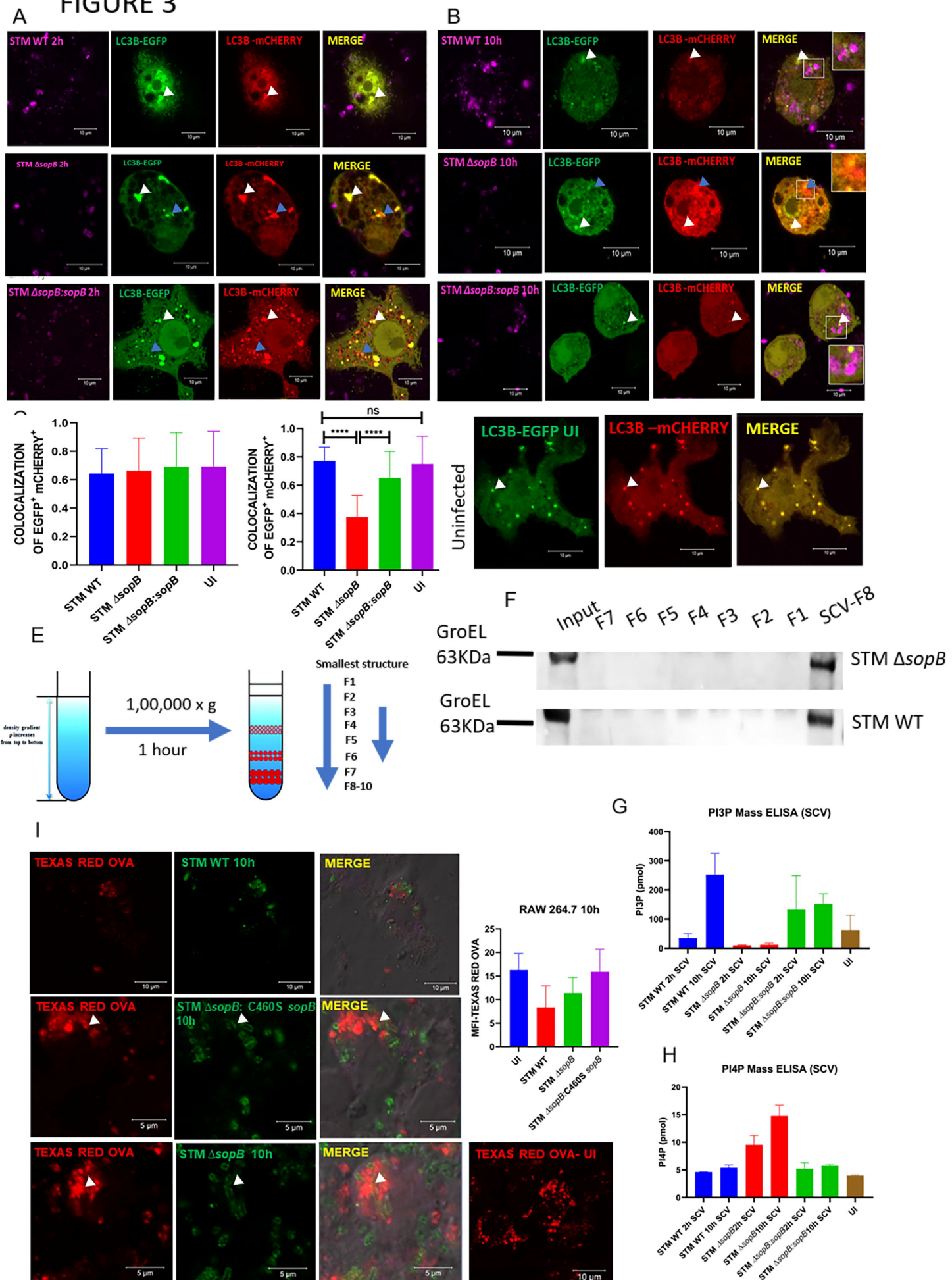
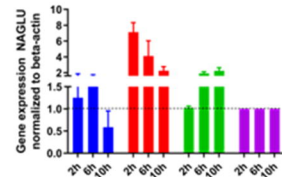


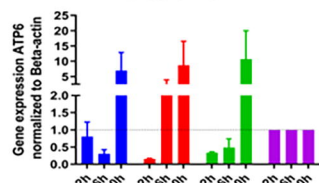
FIGURE 3



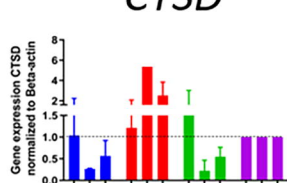
A FIGURE 4 NAGLU



B ATP6

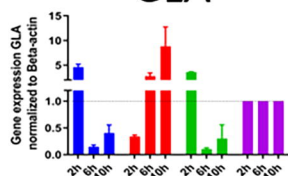


C CTSD



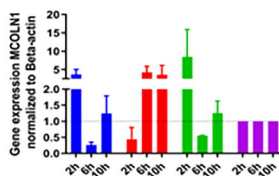
D

GLA

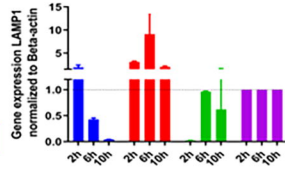


E

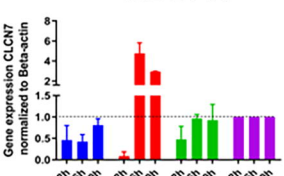
MCOLN1



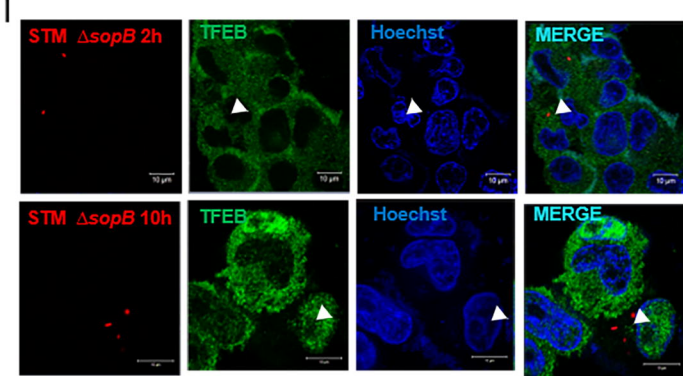
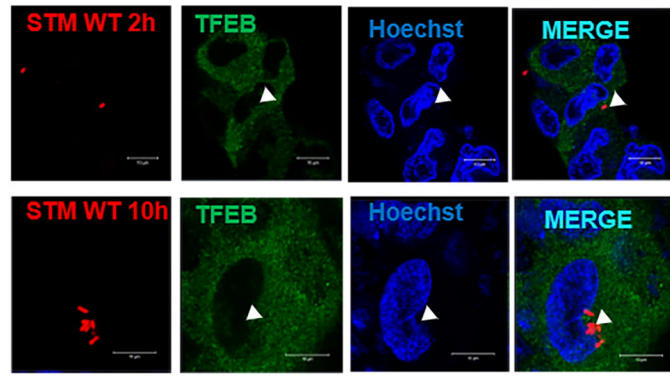
F LAMP1



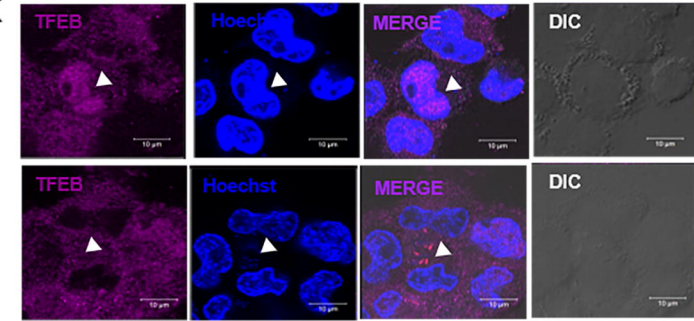
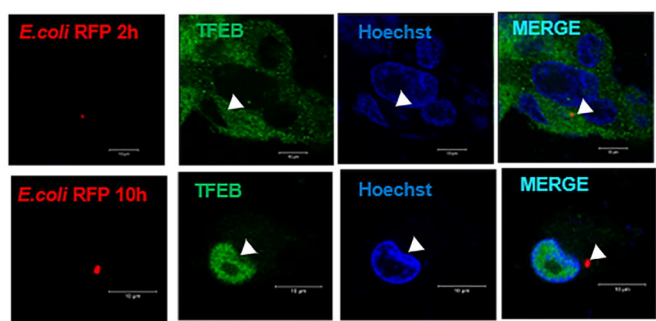
G CLCN7



H

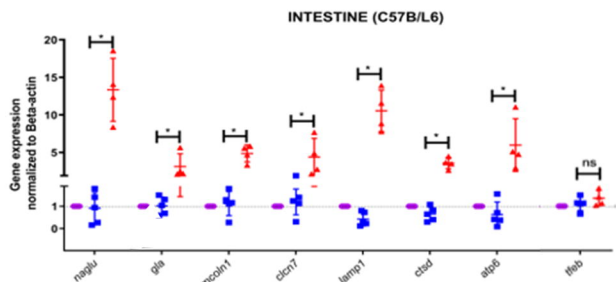


J

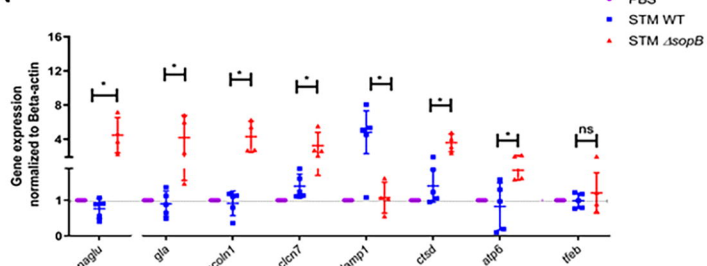


● STM WT
■ STM ΔsopB
▲ STM ΔsopB:sopB

M



N



O

